Photophysical Properties of Core-Modified Expanded Porphyrins: Nature of Aromaticity and Enhancement of Ring Planarity

ARTICLE *in* THE JOURNAL OF PHYSICAL CHEMISTRY B · JULY 2008

Impact Factor: 3.3 · DOI: 10.1021/jp800748n · Source: PubMed

THE JOURNAL OF PHYSICAL CHEMISTRY B

Article

Photophysical Properties of Core-Modified Expanded Porphyrins: Nature of Aromaticity and Enhancement of Ring Planarity

Min-Chul Yoon, Rajneesh Misra, Zin Seok Yoon, Kil Suk Kim, Jong Min Lim, Tavarekere K. Chandrashekar, and Dongho Kim

J. Phys. Chem. B, **2008**, 112 (23), 6900-6905 • DOI: 10.1021/jp800748n • Publication Date (Web): 16 May 2008

ARTICLES

Photophysical Properties of Core-Modified Expanded Porphyrins: Nature of Aromaticity and Enhancement of Ring Planarity

Min-Chul Yoon,[†] Rajneesh Misra,[‡] Zin Seok Yoon,[†] Kil Suk Kim,[†] Jong Min Lim,[†] Tavarekere K. Chandrashekar,*[,‡,§] and Dongho Kim*[,†]

Department of Chemistry, Yonsei University, Seoul 120-749, Korea, Department of Chemistry, Indian Institute of Technology, Kanpur 208016, India, and National Institute for Interdisciplinary Science and Technology, Trivandrum, Kerala 695019, India

Received: January 25, 2008; Revised Manuscript Received: March 17, 2008

We have investigated the excited-state dynamics and nonlinear optical properties of representative core-modified expanded porphyrins, tetrathiarubyrin, tetraselenarubyrin, pentathiaheptaphyrin, tetrathiaoctaphyrin, and tetraselenaoctaphyrin, containing 26, 30, and 34 π electrons using steady-state and time-resolved absorption and fluorescence spectroscopic measurements along with femtosecond Z-scan method, with a particular attention to the photophysical properties related to molecular planarity and aromaticity. Core-modification of macrocycles by sulfur and selenium leads to NIR-extended steady-state absorption and fluorescence spectra and short-lived excited-state due to the heavy-atom effect in time-resolved spectroscopic experiments. Large negative nucleus-independent chemical shift values ranging from −13 to −15 ppm indicate that all molecular systems are highly aromatic. The observed enhancement of two-photon absorption cross-section values over 10^4 GM for core-modified hepta- and octaphyrins is mainly attributable to their rigid and planar structures as well as their aromaticity. Overall, the observed spectroscopic and theoretical results consistently demonstrate the enhanced molecular planarity of core-modified expanded porphyrins compared with their corresponding all-aza expanded porphyrins.

Introduction

Recently, a variety of expanded porphyrin derivatives containing more than four pyrrole rings have been synthesized for diverse applications in medicines, sensors, and catalysts.[1] In parallel with the synthetic approaches, their unique optical properties arising from extended π-conjugation pathways have attracted much attention.[2] Due to the elongated π-conjugation pathways compared to normal tetrapyrrolic macrocycles, expanded porphyrins generally show optical responses in lower energy region. However, as the number of pyrrole rings increases, it has been observed by X-ray crystallography that expanded porphyrins no longer maintain flat structures, resulting in highly distorted 3-dimensional structures, giving rise to somewhat limited elongation of π-conjugation pathway, which is not proportional to the number of pyrrole rings.[3] Especially, *meso*-octakis(pentafluorophenyl) [36]octaphyrin(1.1.1.1.1.1.1.1), a cyclic molecule in which eight pyrrole rings are connected to each other through meso-carbon bridges, exhibits figure-of-eight conformation leading to a loss of aromatic character due to its distorted structure.[3c] β-ethyl-substituted [34]octaphyrin(1.0.1.0.1.0.1.0) also shows similar figure-of-eight structure.[4] In recent years, Sessler and co-workers have reported a successful synthesis of β-ethyl-substituted cyclo[8]pyrrole (formally [30]octaphyrin(0.0.0.0.0.0.0.0)), which does not exhibit distorted conformation.[5] This feature has been attributed to a lack of bridging meso-carbons via direct pyrrole−pyrrole linkages. Nevertheless, the synthesis of planar aromatic octaphyrins remains as a challenge not only from a synthetic viewpoint but also from the point of validity of Hückel's [4n + 2] rule for higher heteroannulene systems.

Third order nonlinear optical response as well as excited-state dynamics in porphyrins-based materials has been an important research topic because of their potential applications such as optical microscopy, 3-D optical memory, and fabrication.[6] In this context, it has been well recognized that two-photon absorption (TPA) processes should be affected by both electronic and structural properties of macrocycles such as effective π-conjugation length, molecular planarity, symmetry, and aromaticity.[3c,7] Thus, it is important to reveal the origin of enhanced TPA cross-section values in terms of a relationship between electronic and geometrical properties since most of expanded porphyrins show large TPA cross-section values. However, photophysical properties for expanded porphyrins as well as core-modified porphyrins have not been widely investigated despite their use in potential applications such as nonlinear optical materials, photodynamic therapy, and multi-anion binding agents.[8]

As continuous efforts on the preparation of planar expanded porphyrins, core-modified octaphyrins (5,14,23,32-tetramesityl-37,40,41,44-tetrathia[34]octaphyrin(1.0.1.0.1.0.1.0) **1** and 5,14,-23,32-tetramesityl-37,40,41,44-tetraselena[34]octaphyrin(1.0.1.0.1.0.1.0) **2**) as well as heptaphyrin (5,10,19,24-tetraphenyl-33,

* To whom correspondence should be addressed. E-mail: dongho@yonsei.ac.kr (D.K.); tkc@iitk.ac.in (T.K.C.).
[†] Yonsei University.
[‡] Indian Institute of Technology.
[§] National Institute for Interdisciplinary Science and Technology.

10.1021/jp800748n CCC: $40.75
Published on Web 05/16/2008

CHART 1: Molecular structures of core-modified expanded porphyrins 1−5

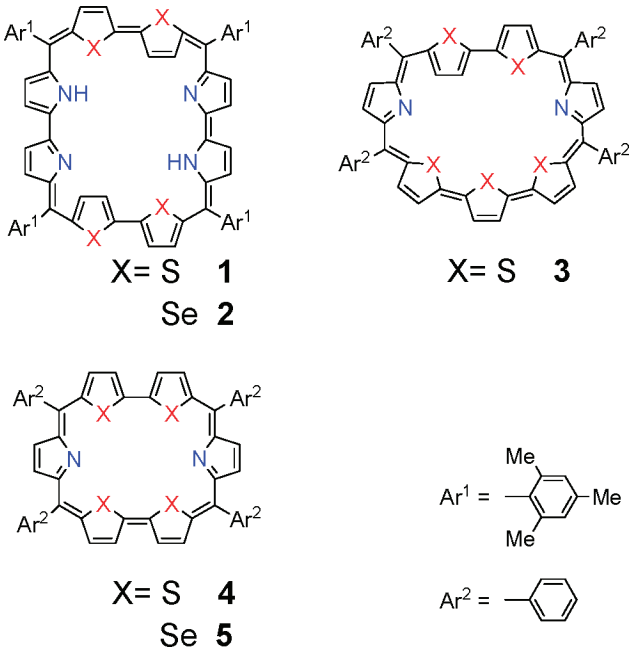

35,36,38,39-pentathia[30]heptaphyrin(1.1.0.1.1.0.0) **3**) and hexaphyrins (5,10,19,24-tetraphenyl-29,31,32,34-tetrathia[26]rubyrin(1.1.0.1.1.0) **4** and 5,10,19,24-tetraphenyl-29,31,32,34-tetraselena-[26]rubyrin **5**) have been recently synthesized by Chandrashekar and co-workers,[9] which revealed the aromatic diatropic ring current effect in ^{1}H NMR spectra, thus providing direct experimental evidence on the validity of Hückel's [4n + 2] rule. In this study, we have investigated the photophysical properties of core-modified expanded porphyrins **1**−**5** (Chart 1) with an emphasis on the structure−property relationship between the planarity and aromaticity of molecules. Specifically, the photophysical properties affected by substituted core-atoms (sulfur and selenium), the number of π-electrons, and cavity sizes have been investigated. With these objectives in mind, various spectroscopic tools such as steady-state absorption and fluorescence, NIR time-resolved fluorescence, femtosecond and nanosecond transient absorption, and femtosecond Z-scan measurements have been utilized for characterization along with the nucleus-independent chemical shift (NICS) calculation. Overall, aromatic planar octaphyrins (**1** and **2**) exhibit NIR-extended steady-state absorption and emission bands, large TPA cross-section values, highly negative NICS(0) values, and relatively short singlet and triplet excited-state lifetimes compared with all-aza octaphyrins. Based on these analyses, we have also investigated the photophysical properties of representative core-modified rubyrins (**4** and **5**) and heptaphyrin (**3**), which show distinctly different photophysical properties. We have also discussed the different heavy-atom effects on their excited-state dynamics between sulfur- and selenium-substituted π-conjugated systems in conjunction with aromaticity and structural planarity.

Experimental Section

Sample Preparation. Synthetic procedures of core-modified expanded porphyrins **1**−**5** are described elsewhere[9] and brief descriptions are given in Supporting Information.

Steady-State Absorption and Emission. Absorption spectra were acquired with a UV−vis spectrometer (Varian, Cary5000). The fluorescence was detected using a near-IR photomultiplier (Hamamatsu, R5108 and H9170−75) and a lock-in amplifier (EG&G, 5210) combined with a chopper after laser excitation at 442 nm from a CW He−Cd laser (Melles Griot, Omnichrome 74). Solvents of HPLC grade were purchased from Sigma-Aldrich Co. and used without further purification. All measurements were carried out at room temperature (23 ± 2 °C).

Time-Resolved Fluorescence. Time-resolved fluorescence was detected using a time-correlated single-photon counting (TCSPC) technique. As an excitation light source, we used a home-built cavity-dumped Ti:sapphire oscillator, which provides a high repetition rate (200−400 kHz) of ultrashort pulses (100 fs of full width at half-maximum (fwhm)) pumped by a CW Nd:YVO4 laser (Spectra-Physics, Millennia V). The output pulses of the oscillator were frequency-doubled with a second-harmonic BBO crystal. The TCSPC detection system consisted of a near-IR photomultiplier (Hamamatsu, H9170-75), a time-to-amplitude converter (TAC, EG&G Ortec, 457), two discriminators (EG&G Ortec, 584 and Canberra, 2126 for signal and trigger, respectively), and two wideband preamplifiers (Philip Scientific and Mini Circuit for signal and trigger, respectively). A personal computer with a multichannel analyzer (Canberra, PCA3) was used for data storage and signal processing. The overall instrumental response function obtained by using an IR dye (Aldrich, IR1100) which has a known lifetime of 6 ps was about 300 ps (fwhm). Quartz cell with optical path length of 10 mm was used for all steady-state experiments and time-resolved fluorescence measurements.

Femtosecond Transient Absorption. The dual-beam femtosecond time-resolved transient absorption spectrometer consisted of two independently tunable homemade noncollinear optical parametric amplifiers (NOPA) pumped by a Ti:sapphire regenerative amplifier system (Spectra-Physics, Hurricane X) operating at 5 kHz repetition rate and an optical detection system. The NOPA systems were based on noncollinearly phase-matching geometry and were easily color tuned by controlling a delay between white light continuum and pump pulses.[10] The generated visible NOPA pulses had a pulse width of 35 fs and an average power of 10 mW at 5 kHz repetition rate in the range 500−700 nm. The probe beam was split into two parts. One part of the probe beam was overlapped with the pump beam at the sample to monitor the transient (signal), while the other part of the probe beam was passed through the sample without overlapping the pump beam to compensate the fluctuation of the probe beam (reference). The time delay between pump and probe beams was carefully controlled by making the pump beam travel along a variable optical delay (Newport, ILS250). To obtain the time-resolved transient absorption difference signal at a specific wavelength, the monitoring wavelength was selected by using an interference filter. By chopping the pump pulses at 131 Hz, the modulated probe−pulses as well as the reference pulses were detected by two separate photodiodes. The modulated signals of the probe−pulses were measured by a gated-integrator (SRS, SR250) and a lock-in amplifier (EG&G, DSP7265) and stored in a personal computer for further signal processing. The polarization angle between pump and probe beam was set at the magic angle (54.7°) in order to prevent polarization-dependent signals. To minimize additional chirp, a quartz cell with 500 μm path length was used, and the overall time-resolution was measured to be less than 40 fs using cross-correlation (fwhm).

Nanosecond Flash Photolysis. Nanosecond transient absorption spectra were obtained using nanosecond flash photolysis methods. Pump pulse with other wavelengths are generated by

optical parametric oscillator (OPO) pumped by third harmonic output of Q-switched Nd:YAG laser (355 nm, Continuum, Surelite II-10). The duration of the excitation pulse was ca. 6 ns, and the pulse energy was ca. 2 mJ/pulse. A CW Xe lamp (150 W) was used as a probe light source for the transient absorption measurement. After passing through the sample, the probe light was collimated and then spectrally resolved using a 15 cm monochromator (Acton Research, SP150) equipped with a 600 grooves/mm grating blazed at 500 nm. The spectral resolution was about 3 nm for a typical transient absorption experiment. The light signal was detected via a photomultiplier tube (Hamamatsu, R928). For the temporal profile measurements, the output signal from the PMT was recorded using a 500 MHz digital storage oscilloscope (Tektronix, TDS3052). Because the triplet state dynamics of molecules in solution are strongly dependent on the dissolved oxygen concentration, efforts were made to remove oxygen rigorously by repeated freeze−pump−thaw cycle. To ensure reproducibility and reliability, the triplet state dynamics of a known standard, Zn(II) tetraphenylporphyrin (Zn(II)TPP), were first recorded in toluene under unaerobic conditions, giving a lifetime of 1 ms at room temperature.[11] Because the concentration of molecules also affects significantly the excited triplet state lifetime (as the result of, e.g., triplet−triplet annihilation processes), efforts were also made to keep the concentration of the samples at or below 10^{-5} M. A relatively low photoexcitation power was also used in order to avoid photodegradation or triplet−triplet annihilation processes.

Femtosecond Z-scan Method. The TPA spectra were measured at 1200−1400 nm by using the open-aperture Z-scan method with ~130 fs pulses from an optical parametric amplifier (Light Conversion, TOPAS), operating at 5 kHz repetition rate pumped by a Ti:sapphire regenerative amplifier system (Spectra-Physics, Hurricane X). The laser beam was divided into two parts. One was monitored by a Ge/PIN photodiode (New Focus) as intensity reference and the other was used for transmittance measurement. The laser beam was focused by $f = 10$ cm lens and transmitted through a quartz cell, whose path length is 1 mm. The position of the sample cell could be varied along the laser-beam direction (z-axis), so the local power density within the sample cell could be changed under a constant laser power level. The transmitted laser beam from the sample cell was then detected by the same photodiode as used for reference monitoring. The on-axis peak intensity of the incident pulses at the focal point, I_0, ranged from 40 to 60 GW/cm^2. Assuming a Gaussian beam profile, the nonlinear absorption coefficient β can be obtained by curve fitting to the observed open-aperture traces with the following equation:[12]

$$T(z) = 1 - \frac{\beta I_0 (1 - e^{-\alpha_0 l})}{2\alpha_0 (1 + (z/z_0)^2)} \quad (1)$$

where α_0 is the linear absorption coefficient, l the sample length, and z_0 the diffraction length of the incident beam. After obtaining the nonlinear absorption coefficient β, the TPA cross-section, $\sigma^{(2)}$ of one solute molecule (in units of 1 GM = 10^{-50} cm^4 s/photon molecule) can be determined by using the following relationship:

$$\beta = \frac{\sigma^{(2)} N_A d \times 10^{-3}}{h\nu} \quad (2)$$

where N_A is the Avogadro constant, d is the concentration of the TPA compound in solution, h is the Planck constant, and ν is the frequency of the incident laser beam. The TPA cross-section $\sigma^{(2)}$ values were measured at wavelengths, where linear absorption is negligible, to satisfy the condition of $\alpha_0 l \ll 1$ in retrieving the pure TPA cross-section $\sigma^{(2)}$ values in the simulation procedure. AF-50 was used as a reference compound which exhibits 50 GM at 800 nm.[13]

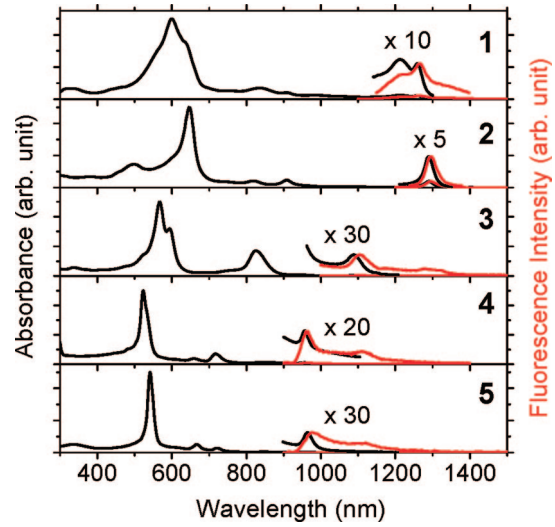

Figure 1. Steady-state absorption (black lines) and fluorescence spectra (red lines) of **1**−**5** in toluene. Fluorescence spectra were measured by photoexcitation with a CW He−Cd laser at 442 nm and monitored at NIR region. Absorption and fluorescence spectra for Q-like bands (900−1400 nm) in all molecules are magnified by the indicated factors.

Quantum Mechanical Calculation and NICS. All Quantum mechanical calculations were performed with the Gaussian 98 program suite.[14] All calculations were carried out by the density functional theory (DFT) method employing the B3LYP level as 6-311+G* basis set. The X-ray crystal structures were used as initial geometry for ground-state geometry optimization. NICS values were obtained by using NMR keyword with same functional and basis set as used in geometry optimization. In these calculations, all peripheral meso-substituents were ignored to reduce hardware resources and simplify assignment the number of π electrons participating in the π-conjugation pathways.

Results and Discussion

Steady-State Absorption and Fluorescence Spectra. The steady-state absorption spectra of **1**−**5** in toluene exhibit two sets of characteristic optical transitions similar to tetrapyrrolic macrocycles such as Zn(II)TPP: high-energy Soret-like bands with strong intensity (~600 nm) and low-energy Q-like bands with relatively weak intensity (1000−1300 nm Figure 1 and Table 1). However, the observed absorption bandwidths are somewhat broad in both regions, compared to Zn(II)TPP, and appear in lower energy, especially for the Q-like bands which extend into NIR region. The red-shift observed in both Soret- and Q-like bands in going from hexaphyrin **4** to octaphyrin **1** is due to elongated effective π-conjugation length as the molecular size increases. In addition, as the core-atoms in thiophene rings are changed from sulfur to selenium, the absorption and fluorescence band maxima are slightly shifted to lower energy regions. Similar red-shifts in chromophores bearing chalcogen atoms were reported by Ohulchanskyy et al.,[15] which shows the same trend as our findings: (1) red-shift in the absorption and emission spectra, (2) decreasing molar extinction coefficient, and (3) increasing intersystem crossing rate in going

TABLE 1: Number of Conjugated π electrons,[a] Band maxima of Absorption and Fluorescence Spectra, Stokes Shifts,[e] Singlet and Triplet Excited-State Lifetimes, TPA Cross-Section Values, and NICS(0) Values[i] of 1−5 in Toluene

molecules	n^a	λ_{abs} (nm)[b,c]	λ_{fl} (nm)[d]	ΔE_{Stokes} (cm^{-1})[e]	τ_S (ps)	τ_T (μs)	$\sigma^{(2)}$ (GM)	NICS(0) (ppm)[i]
1	34	600,[b] 1259[c]	1264	31	10.3[f1]	0.1[g1]	11200[h1]	−13.3
2	34	647,[b] 1289[c]	1296	42	5.9[f2]	0.03[g2]	14700[h2]	−15.1
3	30	568,[b] 1087[c]	1104	142	46.1[f3]	2.7[g3]	15100[h3]	−14.6
4	26	523,[b] 956[c]	960	44	220[f4]	3.9[g4]	2460[h4]	−15.0
5	26	542,[b] 963[c]	970	75	<100[f5]	1.2[g5]	3320[h4]	−15.4

[a] Number of conjugated π-electrons. [b] Absorption wavelength maxima at Soret- and Q-like bands, respectively. [c] Absorption wavelength maxima at Soret- and Q-like bands, respectively. [d] Fluorescence wavelength maxima with photoexcitation at 442 nm. [e] Stokes shifts, that is, energy gaps between absorption (*c*) and fluorescence (*d*) bands of the lowest singlet excited-state (Q(0,0)). [f1] Pumped and probed at 580 and 600 nm, respectively. [f2] Pumped and probed at 580 and 610 nm, respectively. [f3] Pumped and probed at 580 and 580 nm, respectively. [f4] Measured by fluorescence decay using TCSPC. **4** and **5** were excited at 422 nm, and the fluorescence was monitored at several wavelengths from 960 to 970 nm, correspondingly. [f5] Measured by fluorescence decay using TCSPC. **4** and **5** were excited at 422 nm, and the fluorescence was monitored at several wavelengths from 960 to 970 nm, correspondingly. [g1] Pumped and probed at 610 and 500 nm, respectively. [g2] Pumped and probed at 650and 690 nm, respectively. [g3] Pumped and probed at 520and 790 nm, respectively. [g4] Pumped and probed at 530and 500 nm, respectively. [g5] Pumped and probed at 550 and 500 nm, respectively. [h1] Excitation at 1350 nm. [h2] Excitation at 1370 nm. [h3] Excitation at 1220 nm. [h4] Excitation at 1200 nm. [i] Calculated at the ring center, NICS(0).

from O to Se. Furthermore, the extent of red-shift as well as the spectral band shapes in the steady-state absorption spectra becomes manifest in **1** and **2** in comparison with **4** and **5**, implying that the structural changes induced by substitution from sulfur to selenium occur more significantly in the cases of **1** and **2**. In detail, the energy differences between the absorption bands of **1** and **2** are 1211 and 493 cm^{-1} for Soret- and Q-like bands, respectively, which are larger than those for **4** and **5** (670 and 76 cm^{-1} for Soret- and Q-like bands, respectively).

In contrast to **1** and **2**, β-ethyl-substituted all-aza 34-π octaphyrin(1.0.1.0.1.0.1.0) exhibits figure-of-eight molecular conformation, and its Soret- and Q-like bands appear at ~520 nm and ~690 nm, respectively, with a mild dependence on solvents.[4] In addition, meso-substituted all-aza [36]octaphyrin(1.1.1.1.1.1.1.1) shows strong Soret-like band at ~600 nm with featureless Q-like band above ~1000 nm.[3c] However, in the cases of **1** and **2,** the relatively strong and featured absorption bands observed in NIR region suggest that they maintain the molecular planarity even with large cavity size by effective π-electron delocalization, which is also supported by X-ray crystallography and NMR analyses.[16] There are four intramolecular hydrogen-bonding-like interactions corresponding to two N−H···S interactions (R_{H-S} = 3.099 Å) and two βC−H···N interactions (R_{H-N} = 3.378 Å) inside the cavity, and these interactions are presumably responsible for the flat structure observed for **1**. Thus, we suggest that one way to minimize such twisting[3c,4] is to replace a few pyrrole nitrogens by heavier heteroatoms and to increase the steric hindrance around meso-carbons, thereby making meso-substituents more orthogonal to porphyrin plane, such as mesityl groups. Core-modified rubyrins **4** and **5** behave similarly to core-modified octaphyrins, where the absorption and fluorescence band maxima are red-shifted with respect to those of *meso*-tetrakis(pentafluoro-phenyl) [26]rubyrin(1.1.0.1.1.0).[8a,17,18] In addition, all core-modified expanded porphyrins exhibit relatively strong fluorescence in NIR region with photoexcitation at 442 nm. Interestingly, the Stokes shifts for all samples studied here except for **3** are less than 100 cm^{-1}, which are comparatively smaller than those of the corresponding expanded porphyrins, indicating smaller geometrical changes between ground and excited states due to their planar and rigid conformation.[9,16] Furthermore, fluorescence spectrum of core-modified octaphyrin **1** did not show a mirror image of absorption band presumably due to the existence of two conformers in solution corresponding to the results of NMR studies.[16]

Excited Singlet and Triplet State Dynamics. In order to explore the excited-state energy relaxation dynamics of core-modified expanded porphyrins in toluene at room temperature, we have performed time-resolved NIR fluorescence, femtosecond, and nanosecond transient absorption experiments, and the resulting decay parameters are summarized in Table 1. The time-resolved fluorescence decay of **4** revealed the lowest singlet excited-state lifetime of 220 ps that is longer than that of **5** (~100 ps). However, the S_1-state lifetimes of both **4** and **5** are much shorter than that of *meso*-tetrakis(pentafluoro-phenyl) [26]rubyrin(1.1.0.1.1.0) (560 ps).[8a] Likewise, the singlet excited-state lifetime of **1** (10.3 ps) is slightly longer than that of **2** (5.9 ps) obtained by femtosecond transient absorption measurement (Supporting Information). From these results, it is evident that expanded porphyrins substituted by selenium atoms exhibit more conspicuous heavy-atom effect than those substituted by sulfur atoms, which increases the intersystem crossing rate through enhanced spin−orbit coupling.[15] Similar to the case of singlet excited-states, the lifetimes of triplet excited-states are strongly affected by the choice of heteroatoms in pyrrole rings. Specifically, the triplet excited-state lifetime of 3.9 μs was determined for **4,** which is markedly longer than that of **5** (1.2 μs). Similarly, the triplet state lifetime of **1** (100 ns) is longer than that of **2** (30 ns), which can be also interpreted in terms of the heavy-atom effect. An analysis of these data indicates that the observed decrease in the triplet state lifetimes results from the acceleration of intersystem crossing rate for $T_1 \rightarrow S_0$. A similar behavior in the excited-state dynamics was also observed in core-modified tetraphenyl thiaporphyrins.[8b] As the number of sulfur atoms increases in going from H_2TPP to S_2TPP, the excited-state lifetimes in chloroform become shorter with the red-shift of absorption and emission bands (S_1-state lifetimes of 9.5, 1.36, and 1.25 ns and T_1-state lifetimes of 1300, 37.4, and 20.9 μs for H_2TPP, HSTPP, and S_2TPP, respectively). As the number of pyrrole rings increases, both singlet and triplet excited-state lifetimes become shorter in going from **4** to **1**, as well as from **5** to **2**. This feature can be partly explained by acceleration of internal conversion rate (k_{IC}) in terms of both the energy gap law formulated in the following equation and the increase of nonradiative decay channels as the molecular size increases:[19]

$$k_{IC} \sim 10^{13} \exp^{-\alpha \Delta E} \quad (3)$$

where α is a proportionality constant and ΔE is the energy gap between HOMO and LUMO. Since the electronic energy of the lowest excited-state becomes smaller with the delocalization of π-electrons, the internal conversion rates are accelerated as the molecular size increases, which results in shorter excited-state lifetimes.

Two-Photon Absorption Properties and Molecular Structures. To gain further insight into the aromaticity based on Hückel's [4n + 2] rule of π-conjugated molecular systems,[8a,20,21] we have measured the TPA cross-section values of **1**−**5** by using femtosecond Z-scan measurement in conjunction with molecular planarity and the number of π electrons in core-modified expanded porphyrin systems. We have selected two-photon excitation wavelengths, where one-photon absorption contribution to two-photon absorption could be ignored. As a result, **1**−**3** show much larger TPA cross-section values (over 10^4 GM) compared with smaller macrocycle systems, **4** and **5** (see Table 1 and Supporting Information). Especially, the TPA cross-section values of **1** and **2** are larger than those of the corresponding expanded porphyrins containing eight pyrrole rings. For instance, the TPA cross-section value of [36]octaphyrin(1.1.1.1.1.1.1.1) was measured to be 870 GM and that of cyclo[8]pyrrole was found to be 3030 GM with the two-photon excitation wavelengths at 1240 and 1600 nm, repectively.[3c,8a] We think that the planarity and the molecular shape (ratio of long molecular axis to short axis) are mainly responsible for these differences in the TPA cross-section values. [36]octaphyrin(1.1.1.1.1.1.1.1) shows highly distorted figure-of-eight structure and cyclo[8]pyrrole shows highly symmetric circular shape. In our previous reports, we observed much larger TPA values in the linearly linked fused porphyrin arrays than those in the two-dimensionally connected square-shape porphyrin array.[21a,22] Thus, we can suggest that the large TPA cross-section values in core-modified expanded porphyrin systems originated from planar geometries and rectangular molecular shapes. In other words, the directionality in molecular polarizability is another important parameter for the enhancement of TPA cross-section values in addition to the number of π electrons and the planar structures of π-conjugated cyclic molecules.[8a] Additionally, the enhanced molecular rigidity by hydrogen-bonding-like interactions in **1** and **2** is conceived to increase the TPA cross-section values.[9,16] In spite of planar geometries, the TPA cross-section values of core-modified rubyrins (~3000 GM for **4** and **5**) are much smaller than that of all-aza rubyrin (9080 GM),[8a] presumably because the wavelength for TPA spectra could not reach the maxima of Soret-like absorption bands due to our experimental limit in the cases of **4** and **5**.

Relationship between Aromaticity and Two-photon Absorption Properties. It is now generally accepted that among various indices of aromaticity the nucleus-independent chemical shift (NICS) value, reflecting magnetic shielding/deshielding by induced π-electronic ring current, is one of the most appropriate methods to describe aromatic nature of π-conjugated cyclic molecular systems, such as expanded porphyrins.[8a,23,24] For the quantitative evaluation of aromaticity, we have calculated the NICS(0) values at the center of molecular plane with optimized geometry using quantum mechanical calculation at B3LYP/6-311+G* level. Concurrent with [4n + 2] π electrons on the π-conjugation pathways, the NICS(0) calculations show large negative values ranging from −13.3 to −15.4 ppm for **1**−**5**, which exhibits efficient diatropic ring current (Table 1). Compared with distorted expanded porphyrins, these large negative NICS(0) values indicate that the core-modified expanded porphyrins are highly aromatic with relatively flat structures. In particular, larger NICS(0) values in **1** and **2** are mainly due to their increased hydrogen-bonding-like interactions inside the cavity upon substitution of pyrrole nitrogens with sulfur and selenium atoms.

According to our recent investigations on the relationship between aromaticity and nonlinear optical response of various expanded porphyrins, the TPA cross-section values are partly proportional to the aromaticity of molecules.[3c,8a,21b,25] Especially, the electronic nature of molecular system mainly determines the TPA efficiency in porphyrin systems, when two-photon excitations near Soret-like bands are considered. The TPA cross-section values for aromatic bisgold coordinated [26]hexaphyrins are five times larger than those of antiaromatic bisgold coordinated [28]hexaphyrins with various substituents.[25] As compared with antiaromatic compounds, their corresponding aromatic congeners have distinct NIR-extended Q-like bands due to well-defined HOMO−LUMO transitions. It was found that relatively intense and red-shifted Q-like bands can act as an intermediate state in the three-state model, which describes well two-photon transition processes based on the second-order perturbation theory as follows.[6]

$$\sigma^{(2)} = 2\frac{(2\cos^2\theta + 1)}{15}\frac{(2\pi)^2\nu^2L^4}{(hc)^2n^2}\frac{|\mu_{i0}|^2|\mu_{fi}|^2}{(\nu_{i0} - \nu)^2 + (\Gamma_i/2)^2}g(2\nu) \quad (4)$$

where $\sigma^{(2)}$ is the TPA cross-section value, n is the refractive index of solvent medium, L is Lorentz local field factor, calculated as $L = (n^2 + 2)/3$, μ_{i0} (μ_{fi}) is the transition dipole moment for the electronic transition between intermediate and initial (final) states, θ is the angle between transition dipole moments μ_{i0} and μ_{fi}, ν_{io} is the energy gap between intermediate and ground states, ν is laser frequency, Γ_i is the line-width of ith state, and $g(2\nu)$ is the normalized TPA line shape function. As per eq 4, the TPA cross-section values increase as the energy of intermediate state becomes closer to the laser frequency ν and the transition dipole moments involving ith state become larger. Thus, the enhancement of TPA cross-section values in aromatic molecules mainly comes from the role of Q-like states acting as the ladder intermediate state. Although we could not compare the results of aromatic core-modified expanded porphyrins with those of their antiaromatic congeners in this study, it is believed that the observed large TPA cross-section values for **1**−**5** should be a result of their aromatic nature. From these results, it is concluded that the efficiency of TPA processes is governed by both electronic and structural properties such as aromaticity and molecular planarity.

Conclusions

The substitution of pyrrole nitrogens with sulfur and selenium atoms provides increased intramolecular hydrogen-bonding-like interactions inside the cavity, leading to more flat geometry compared with the corresponding all-aza expanded porphyrins. Based on the steady-state absorption and fluorescence spectral features observed in NIR region, the large TPA cross-section values and the quantitative analyses of aromaticity using NICS calculation, we can suggest that **1** and **2** sustain flat structures by heavier heteroatoms. It should be noted that the maintenance of structural planarity in expanded porphyrins plays an important role in the elongation of π-conjugation pathway, which can be well correlated with optical nonlinear properties. Overall, our current study demonstrates a good correlation between aromaticity and TPA, suggesting that the TPA cross-section values can serve as a quantitative measure of aromaticity especially in large π-conjugated cyclic molecular systems.

Acknowledgment. The work at Yonsei University was financially supported by the Star Faculty and BK21 Programs of the Ministry of Education and Human Resources of Korea. M.-C.Y., Z.S.Y., K.S.K., and J.M.L. acknowledge the fellowship

of the BK21 program from the Ministry of Education and Human Resources Development of Korea. T.K.C. thanks the Department of Science and Technology for a J. C. Bose fellowship. R.M. thanks the Council of Scientific and Industrial Research, New Delhi for a SRF fellowship of India.

Supporting Information Available: Details of sample preparation, time-resolved fluorescence data, femtosecond and nanosecond transient absorption decay profiles, and open-aperture femtosecond Z-scan data. This material is available free of charge via the Internet at http://pubs.acs.org.

References and Notes

(1) (a) Jasat, A; Dolphin, D *Chem. Rev* **1997**, *97*, 2267. (b) Furuta, H.; Maeda, H; Osuka, A. *Chem. Commun.* **2002**, 1795. (c) Sessler, J. L.; Seidel, D. *Angew. Chem., Int. Ed.* **2003**, *42*, 5134.

(2) (a) Weghorn, S. J.; Sessler, J. L.; Lynch, V.; Baumann, T. F.; Sibert, J. W. *Inorg. Chem.* **1996**, *35*, 1089. (b) Anand, V. G.; Saito, S.; Shimizu, S.; Osuka, A. *Angew. Chem., Int. Ed.* **2005**, *44*, 7244.

(3) (a) Misra, R.; Chandrashekar, T. K. *Acc. Chem. Res.* **2008**, *41*, 265. (b) Shin, J.-Y.; Furuta, H.; Yoza, K.; Igarashi, S.; Osuka, A. *J. Am. Chem. Soc.* **2001**, *123*, 7190. (c) Tanaka, Y.; Saito, S.; Mori, S.; Aratani, N.; Shinokubo, H.; Shibata, N.; Higuchi, Y.; Yoon, Z. S.; Kim, K. S.; Noh, S. B.; Park, J. K.; D; Kim; Osuka, A. *Angew. Chem., Int. Ed.* **2008**, *47*, 681.

(4) (a) Bröring, A.; Jendrny, J.; Zander, L.; Schmickler, H.; Lex, J.; Wu, Y.-D.; Nendel, M.; Chen, J.; Plattner, D. A.; Houk, K. N.; Vogel, E. *Angew. Chem., Int. Ed.* **1995**, *34*, 2515. (b) Bley-Escrich, J.; Gisselbrecht, J.-P.; Vogel, E.; Gross, M. *Eur. J. Chem.* **2002**, 2829. (c) Lintuluoto, J. M.; Nakayama, K.; Setsune, J. *Chem. Commun.* **2006**, 3492.

(5) (a) Baker, E. S.; Lee, J. T.; Sessler, J. L.; Bowers, M. T. J. Am. Chem. Soc. 2006, 128, 2641. (b) Kohler, T.; Seidel, D.; Lynch, V.; Arp, F. O.; Ou, Z.; Kadish, K. M.; Sessler, J. L. *J. Am. Chem. Soc.* **2003**, *125*, 6872.

(6) (a) Drobizhev, M.; Stepanenko, Y.; Dzenis, Y.; Karotki, A.; Rebane, A.; Taylor, P. N.; Anderson, H. L. *J. Phys. Chem. B.* **2005**, *109*, 7223. (b) Drobizhev, M.; Stepanenko, Y.; Rebane, A.; Wilson, C. J.; Screen, T. E. O.; Anderson, H. *J. Am. Chem. Soc.* **2006**, *128*, 12432.

(7) (a) Kurotobi, K.; Kim, K. S.; Noh, S. B.; Kim, D.; Osuka, A. *Angew. Chem., Int. Ed.* **2006**, *45*, 3944. (b) Ahn, T. K.; Kim, K. S.; Kim, D. Y.; Noh, S. B.; Aratani, N.; Ikeda, C.; Osuka, A.; Kim, D. *J. Am. Chem. Soc.* **2006**, *128*, 1700.

(8) (a) Yoon, Z. S.; Kwon, J. H.; Yoon, M.-C.; Koh, M. K.; Noh, S. B.; Sessler, J. L.; Lee, J. T.; Seidel, D.; Aguilar, A.; Shimizu, S.; Suzuki, M.; Osuka, A.; Kim, D. *J. Am. Chem. Soc.* **2006**, *128*, 14128. (b) Srinivasan, A.; Kumar, M. R.; Pandian, R. P.; Mahajan, S.; Pushpan, S.; Sridevi, B.; Narayanan, S. J.; Chandrashekar, T. K. *J. Porphyrins Phthalocyanines* **1998**, *2*, 305.

(9) (a) Chandrashekar, T. K.; Venkatraman, S. *Acc. Chem. Res.* **2003**, *36*, 676. (b) Pushpan, S. K.; Chandrashekar, T. K *Pure Appl. Chem.* **2002**, *74*, 2045.

(10) Cerullo, G.; Nisoli, M.; Stagira, S.; Silvestri, S. De. *Opt. Lett.* **1998**, *23*, 1283.

(11) Kalyanasundaram, K. *Photochemistry of Polypyridine and Porphyrin Complexes*; Academic Press: New York, 1991.

(12) Sheik-Bahae, M.; Said, A. A.; Wei, T.-H.; Hagan, D. G.; van Stryland, E. W. *IEEE J. Quantum Electron.* **1990**, *26*, 760.

(13) Kim, O. K.; Lee, K. S.; Woo, H. Y.; Kim, K. S.; He, G. S.; Swiatkiewicz, J.; Prasad, P. N. *Chem. Mater.* **2000**, *12*, 284.

(14) Frisch, M. J.; Trucks, G. W.; Schlegel, H. B.; Scuseria, G. E.; Robb, M. A.; Cheeseman, J. R.; Zakrzewski, V. G.; Montgomery, J. A., Jr.; Stratmann, R. E.; Burant, J. C.; Dapprich, S.; Millam, J. M.; Daniels, A. D.; Kudin, K. N.; Strain, M. C.; Farkas, O.; Tomasi, J.; Barone, V.; Cossi, M.; Cammi, R.; Mennucci, B.; Pomelli, C.; Adamo, C.; Clifford, S.; Ochterski, J.; Petersson, G. A.; Ayala, P. Y.; Cui, Q.; Morokuma, K.; Malick, D. K.; Rabuck, A. D.; Raghavachari, K.; Foresman, J. B.; Cioslowski, J.; Ortiz, J. V.; Stefanov, B. B.; Liu, G.; Liashenko, A.; Piskorz, P.; Komaromi, I.; Gomperts, R.; Martin, R. L.; Fox, D. J.; Keith, T.; Al-Laham, M. A.; Peng, C. Y.; Nanayakkara, A.; Gonzalez, C.; Challacombe, M.; Gill, P. M. W.; Johnson, B. G.; Chen, W.; Wong, M. W.; Andres, J. L.; Head-Gordon, M.; Replogle, E. S.; Pople, J. A. Gaussian 98, revision A.11; Gaussian, Inc.: Pittsburgh, PA, 1998.

(15) (a) Ohulchanskyy, T.; Donnelly, D. J.; Detty, M. R.; Prasad, P. N. *J. Phys. Chem. B* **2004**, *108*, 8668. (b) Detty, R.; Merkel, P. B. *J. Am. Chem. Soc.* **1990**, *112*, 3845.

(16) Anand, V. G.; Pushpan, S. K.; Venkatraman, S.; Dey, A.; Chandrashekar, T. K.; Joshi, B. S.; Roy, R.; Teng, W.; Senge, K. R. *J. Am. Chem. Soc.* **2001**, *123*, 8620.

(17) Narayanan, J. S.; Srinivasan, A.; Sridevi, B.; Chandrashekar, T. K.; Senge, M. O.; Sugiura, K.; Sakata, Y. *Eur. J. Org. Chem.* **2000**, 2357.

(18) Band maxima of absorption and fluorescence spectra of all-aza rubyrin are 543 (Soret), 926 (Q), and 968 nm (emission) in toluene.

(19) Turro, N. J. *Modern Molecular Photochemistry*; The Benjamin/Cummings Publishing Co.: Menlo Park, 1978; pp 180−195.

(20) Kwon, J. H.; Ahn, T. K.; Yoon, M.-C.; Kim, D. Y.; Koh, M. K.; Kim, D.; Furuta, H.; Suzuki, M.; Osuka, A. *J. Phys. Chem. B* **2006**, *110*, 11683.

(21) (a) Nakamura, Y.; Aratani, N.; Shinokubo, H.; Takagi, A.; Kawai, T.; Matsumoto, T.; Yoon, Z. S.; Kim, D. Y.; Ahn, T. K.; Kim, D.; Muranaka, A.; Kobayashi, N.; Osuka, A. *J. Am. Chem. Soc.* **2006**, *128*, 4119. (b) Ahn, T. K.; Kwon, J. H.; Kim, D. Y.; Cho, D. W.; Jeong, D. H.; Kim, S. K.; Suzuki, M.; Shimizu, S.; Osuka, A.; Kim, D. *J. Am. Chem. Soc.* **2005**, *127*, 12856.

(22) Yoon, M.-C.; Noh, S. B.; Tsuda, A.; Nakamura, Y.; Osuka, A.; Kim, D. *J. Am. Chem. Soc.* **2007**, *129*, 10080.

(23) Sessler, J. L.; Cho, D.-G.; Stêpieñ, M.; Lynch, V.; Waluk, J.; Yoon, Z. S.; Kim, D. *J. Am. Chem. Soc.* **2006**, *128*, 12640.

(24) Chen, Z.; Wannere, C. S.; Corminboeuf, C.; Puchta, R.; Schleyer, P. v. R. *Chem. Rev.* **2005**, *105*, 3842.

(25) Mori, S.; Kim, K. S.; Yoon, Z. S.; Noh, S. B.; Kim, D.; Osuka, A. *J. Am. Chem. Soc.* **2007**, *129*, 11344.

JP800748N